

METHODOLOGY

Open Access



# Estimation of nitrate nitrogen content in cotton petioles under drip irrigation based on wavelet neural network approach using spectral indices

Zhiqiang Dong<sup>1,2</sup>, Yang Liu<sup>1,2\*</sup>, Baoxia Ci<sup>1,2</sup>, Ming Wen<sup>1,2</sup>, Minghua Li<sup>1,2</sup>, Xi Lu<sup>1,2</sup>, Xiaokang Feng<sup>1,2</sup>, Shuai Wen<sup>1,2</sup> and Fuyu Ma<sup>1,2\*</sup>

## Abstract

**Background:** Estimation of nitrate nitrogen ( $\text{NO}_3^-$ -N) content in petioles is one of the key approaches for monitoring nitrogen (N) nutrition in crops. Rapid, non-destructive, and accurate evaluation of  $\text{NO}_3^-$ -N contents in cotton petioles under drip irrigation is of great significance.

**Methods:** In this study, we discussed the use of hyperspectral data to estimate  $\text{NO}_3^-$ -N contents in cotton petioles under drip irrigation at different N treatments and growth stages. The correlations among trilateral parameters and six vegetation indices and petiole  $\text{NO}_3^-$ -N contents were first investigated, after which a traditional regression model for petioles  $\text{NO}_3^-$ -N content was established. A wavelet neural network (WNN) model for estimating petiole  $\text{NO}_3^-$ -N content was also established. In addition, the performance of WNN was compared to those of random forest (RF), radial basis function neural network (RBF) and back propagation neural network (BP).

**Results:** Between the blue edge amplitude (Db) and blue edge area (SDb) of the blue edge parameters was the optimal index for the estimation model of petiole  $\text{NO}_3^-$ -N content. We found that the prediction results of the blue edge parameters and WNN were 7.3% higher than the coefficient of determination ( $R^2$ ) of the first derivative vegetation index and WNN. Root mean square error (RMSE) and mean absolute error (MAE) were 25.2% and 30.9% lower than first derivative vegetation, respectively, and the performance was better than that of RF, RBF and BP.

**Conclusions:** An inexpensive approach consisting of the WNN algorithm and blue edge parameters can be used to enhance the accuracy of  $\text{NO}_3^-$ -N content estimation in cotton petioles under drip irrigation.

**Keywords:** Nitrate nitrogen, Cotton, Petiole, Remote sensing, Wavelet neural network

## Background

Optimal management of nitrogen (N) fertilizer is important to in the improvement of cotton yield and quality [1], as well as in the reduction of waste and environmental

problems associated with excess N fertilizer input [2]. A reasonable amount of N fertilizer is conducive for the balance between vegetative growth in cotton, and promotion of N absorption as well as utilization [3, 4]. The N fertilizer is generally stored and assimilated by cotton plants in the form of nitrate nitrogen ( $\text{NO}_3^-$ -N).  $\text{NO}_3^-$ -N contents vary in different parts of the cotton plant in the order of petioles > stems > leaves [5, 6]. Therefore, petiole  $\text{NO}_3^-$ -N content is an effective parameter

\*Correspondence: ly0318@163.com; mfy\_agr@shzu.edu.cn

<sup>1</sup> School of Agriculture, Shihezi University, Shihezi 832003, Xinjiang, People's Republic of China

Full list of author information is available at the end of the article



© The Author(s) 2021. **Open Access** This article is licensed under a Creative Commons Attribution 4.0 International License, which permits use, sharing, adaptation, distribution and reproduction in any medium or format, as long as you give appropriate credit to the original author(s) and the source, provide a link to the Creative Commons licence, and indicate if changes were made. The images or other third party material in this article are included in the article's Creative Commons licence, unless indicated otherwise in a credit line to the material. If material is not included in the article's Creative Commons licence and your intended use is not permitted by statutory regulation or exceeds the permitted use, you will need to obtain permission directly from the copyright holder. To view a copy of this licence, visit <http://creativecommons.org/licenses/by/4.0/>. The Creative Commons Public Domain Dedication waiver (<http://creativecommons.org/publicdomain/zero/1.0/>) applies to the data made available in this article, unless otherwise stated in a credit line to the data.

that reflects overall N nutrition status of cotton, and petioles can be used as primary plant parts for diagnosing N nutrition [7–9]. Petioles also facilitate rapid determination of N nutrition status of plants to guide rational N fertilizer application [10, 11].

The traditional methods for evaluating cotton N nutrition include soil mineral N determination, laboratory analysis of the plant and determination of petiole  $\text{NO}_3^-$ -N levels among others [12, 13]. However, these methods are associated with certain limitations such as cumbersome procedures, that are time consuming, poor timing of analyses results, and they also involve destructive sampling of many plants [14, 15]. Due to its non-destructive, cheap, and efficient characteristics, hyperspectral remote sensing technology has been used to estimate physiological parameters during crop growth and development [16]. Diagnosis of N nutrition in crops based on spectral data has made considerable progress [17]. The technique has been applied in several crops to obtain crop N nutrition status spectral indices [18–20]. Based on spectral indices, various crop N nutrition monitoring models have been established, and they have achieved a high accuracy. Abulaiti et al. [21] proposed a novel approach for characterizing the Total Nitrogen Content (TNC) by canopy spectral reflectance through a fractional order derivative (FOD) and optimized spectral indices (NDSI, RSI). Rao et al. [22] confirmed the potential of the EO-1 Hyperion hyperspectral sensor for the estimation of total chlorophyll and nitrogen concentrations in cotton crops by developing regression models between hyperspectral reflectance and laboratory measurements of leaf total chlorophyll and nitrogen concentrations. Studies on hyperspectral estimation of  $\text{NO}_3^-$ -N content are limited and most of which focus on plant N content. Gautam et al. [23] used two neural network architectures (Back Propagation and Radial Basis Function) were used to develop twenty different models to predict corn crop  $\text{NO}_3^-$ -N content. They found that radial basis function model based on green vegetation index textural features provided the best performance with an average accuracy of 92.1%.

In addition, parameters associated with spectral location characteristics, trilateral parameters reflect spectral characteristics of vegetation and are also sensitive to variations in N content [24]. The red edge parameter, which is one of the trilateral parameters has been used to estimate N nutrition various crops with satisfactory outcomes [25, 26]. The red edge blue shift phenomenon exists in reflectance spectra of numerous crops. Railyan [27] and Gilbert [28] established that the position and red edge slope in triticale and maize constantly varied during the entire growing season, and were closely associated with the phenological period of crops. The red

edge shifted to the long wave direction in the vegetative growth stage, and shifted to the short wave direction in the reproductive growth stage.

Spectral indices of crops can be obtained by developing linear or non-linear relationships or by the learning method of artificial neural networks. Spectral indices combined with artificial neural network algorithms have been used to estimate N contents. Based on adaptive differential optimization extreme learning machine, radial basis function (RBF) and particle swarm optimization BP, Feng et al. [29] established quantitative estimation models for N content estimation in rice canopy leaves. To rapidly and accurately estimate N contents in maize in natural environments, Xiu et al. [30] proposed a method for measuring maize N content based on wavelet energy coefficient and back propagation neural network (BP). Compared to the regression analysis model, the method improved the accuracy of corn N content estimation. Wavelet neural network (WNN) [31] is a type of artificial neural network, that is generated by applying wavelet analysis theory to neural network theory. This network exhibits strong non-linear mapping and learning abilities [31]. Current studies on WNN traverse several fields, including medicine [32], industry [33], and finance [34] and has achieved satisfactory results.

Determination of  $\text{NO}_3^-$ -N content in plants during the growing season for N nutrition monitoring is common in Europe [35]. In China, there are related applications in wheat [36] and corn [37], but less in cotton. Few studies have evaluated the efficacy of the hyperspectral technology to monitor  $\text{NO}_3^-$ -N contents in cotton petioles. A combined WNN model, which has strong adaptive and fault tolerant abilities, can effectively estimate the advantages of linear and nonlinear functions, and facilitate the estimation of petiole  $\text{NO}_3^-$ -N contents in cotton under drip irrigation to provide technical references for cotton growth and N nutrition diagnosis under drip irrigation. Therefore, in this study, we selected spectral indices and trilateral parameters that are sensitive to N and used them to estimate the  $\text{NO}_3^-$ -N content of cotton petioles based on experimental cotton conditions such as drip irrigation, and various N application levels in Xinjiang.

## Methods

### Experimental design

The field experiment was performed in 2019 at the teaching experiment farm of Shihezi University, Shihezi City, Xinjiang Uygur Autonomous Region (86° 02' E, 44° 18' N) (Fig. 1a, b). Soil fertility of the 0–20 cm soil layer in the experimental plots was determined; total N was 1.13 g/kg, alkali-hydro N was 44.26 mg/kg, available phosphorus content was 19 mg/kg, available potassium content was 486 mg/kg, organic matter content was 15.50 g/kg, while

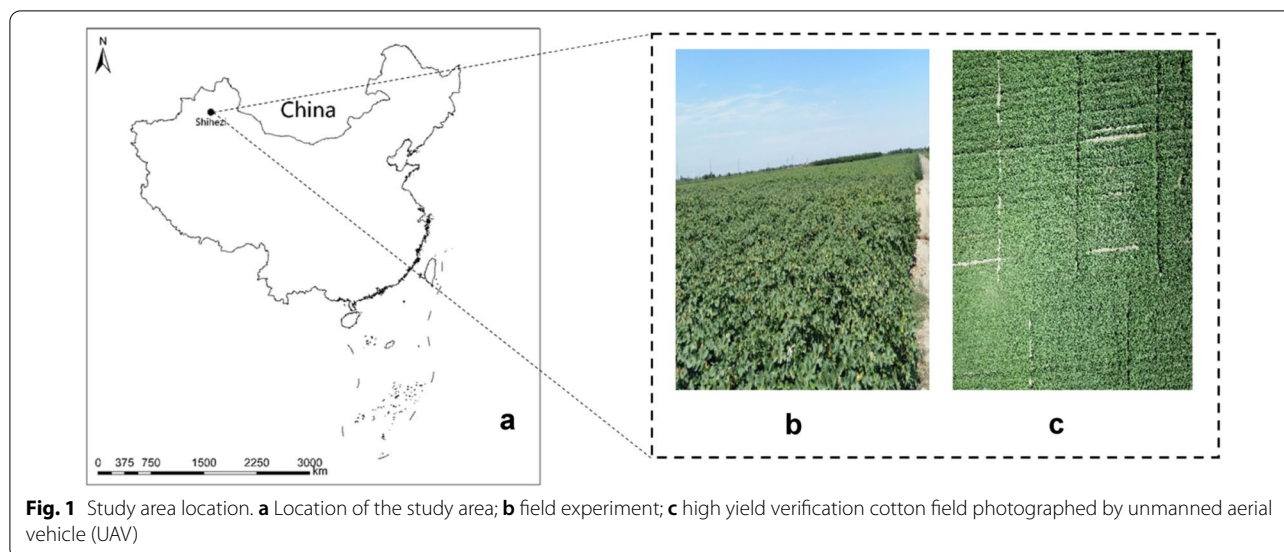


**Fig. 1** Study area location. **a** Location of the study area; **b** field experiment; **c** high yield verification cotton field photographed by unmanned aerial vehicle (UAV)

the pH was 8.17. The Lumianyan 24 cotton variety, which is a middle-late maturing variety, with a growth period of approximately 130 days was used as the experiment material. Lumianyan 24 was planted on 23rd April and was harvested on 5th October in 2019.

Five N rates were designed as follows: 0 kg/ha (N0), 195.5 kg/ha (N1), 299 kg/ha (N2), 402.5 kg/ha (N3) and 506 kg/ha (N4). Total amounts of phosphate ( $P_2O_5$ ) and potassium ( $K_2O$ ) fertilizers were 109.8 kg/ha and 91.8 kg/ha, respectively. One film, three rows, and three belts were used in the experiment. Row spacing was 76 cm while plant spacing was 10 cm. Each treatment was performed in triplicate and arranged in completely randomized blocks covering a plot area of 2.25 m  $\times$  15 m. Cotton was first grown in the experimental field after which protective rows were set around the cotton plants. Other field management measures were in accordance with the requirements of high-yield cultivation. Fertilizers were applied with irrigation water during the cotton growth period under drip irrigation with film.

Validation test data were obtained from a high-yield cotton field in Shihezi university teaching experimental field (Fig. 1c). The independent test cotton field was divided into 15 plots. The total amounts of N fertilizer applied was 300 kg/ha, while total amount of  $P_2O_5$  and  $K_2O$  fertilizers applied were 109.8 kg/ha and 91.8 kg/ha, respectively.

#### Spectral data acquisition

Key growth periods of cotton were defined as follows: full bud period (65 days after sowing), initial flowering period (77 days after sowing), full flowering period (88 days after sowing), and initial boll stage (107 days after sowing). The

analytical spectral devices (ASD) FieldSpec 3 portable spectrometer (Analytical Spectral Devices Inc., Boulder, CO, Colorado, USA) was used to obtain spectral data of the cotton canopy. The band range was 350–1075 nm while the field of view was 25°. Three rows of cotton plants with uniform growth in different treatment plots were randomly selected. The spectrometric probe was vertically placed downward at 25 cm above the canopy. The trigger was pulled during scanning and the obtained spectral data automatically saved. Spectral data acquisition time was three hours. Average values of the three curves were calculated using the Viewspec software (Analytical Spectral Devices, Inc., Boulder, CO, Colorado, USA) as reflectance values of cell spectra.

#### Determination of $NO_3^-$ -N content in cotton petioles


After the collection of canopy spectral data, 20 cotton plants with petioles (10 days after topping) and two leaves (10 days after topping) were randomly selected from the experimental plots. Cotton petioles and leaves were separated. Petioles were cut and pressed, and the sap was immediately measured using the LAQUA twin  $NO_3^-$  meter (HORIBA Inc., Japan). The LAQUA twin  $NO_3^-$  meter is a rapid and effective method for evaluating nitrogen levels. The test process, which is widely used in crops nitrogen diagnosis, is simple and accurate [35, 37]. A brief description of  $NO_3^-$  meter is presented in Table 1.

#### Spectral parameter selection

Spectral indices were associated with cotton photosynthesis, soil fertility level, and nutrient management among others. Six spectral indices and trilateral

**Table 1** LAQUA twin NO<sub>3</sub><sup>-</sup>-N instrument profile

Instruments name	LAQUA twin NO <sub>3</sub> <sup>-</sup>
Measuring principles	Ion electrode
Volume of samples required	0.3–2.0 mL
Scope of measurement	2–9900 mg/L



parameters that are sensitive to N nutrition in cotton under drip irrigation were selected based on spectral response characteristics of cotton canopy under drip irrigation and previous studies, as shown in Table 2.

WNN was used to establish the estimation model of cotton petiole NO<sub>3</sub><sup>-</sup>-N contents. Two spectral characteristic indices and two trilateral parameters with strong correlations between critical growth period and petiole NO<sub>3</sub><sup>-</sup>-N content were selected as independent variables to develop a cotton petiole NO<sub>3</sub><sup>-</sup>-N content model. Independent validation samples were used to test the regression model. The coefficient of determination (R<sup>2</sup>), root mean square error (RMSE), and mean absolute error (MAE) were used to enhance the accuracy of the model to develop the best estimation model (Eqs. 1–3). Mean

relative error (MRE) was used to determine the number of hidden nodes in WNN (Eq. 4).

$$R^2 = 1 - \frac{\sum_{i=1}^n (F_i - T_i)^2}{\sum_{i=1}^n (T_i - \bar{T}_i)^2}; \tag{1}$$

$$RMSE = \sqrt{\frac{1}{n} \times \sum_{i=1}^n (F_i - T_i)^2}; \tag{2}$$

$$MAE = \frac{1}{n} \sum_{i=1}^n |F_i - T_i|; \tag{3}$$

$$MRE = \sqrt{\frac{1}{n} \times \sum_{i=1}^n \left(\frac{F_i - T_i}{T_i}\right)^2} \times 100\%; \tag{4}$$

whereby, F<sub>i</sub> and T<sub>i</sub> are the predicted and true values, respectively, while n is the number of samples.

**Modeling methods**

WNN [46] is an artificial neural network that is based on wavelet analysis. The S-type activation function of the hidden node in the neural network is replaced with the wavelet function. The corresponding weight from the input layer to the hidden layer, and the threshold value of the hidden layer are replaced with scale expansion and time shift factors of wavelet function, respectively.

Determination of the number of hidden layer nodes is a key factor influencing the accuracy of the WNN prediction model. Therefore, the number of hidden layer nodes is determined under the condition of meeting model accuracy while the compactness of the model structure is ensured to avoid redundancy. In the present

**Table 2** Calculation methods and reflectance of spectral indices

Spectral index	Abbreviation	Formula	References	
Trilateral parameters	Red edge amplitude	Dr	Maximum first derivative within 680–760	[38]
	Red edge area	SDr	Sum of first derivative values in red edge	[38]
	Yellow edge amplitude	Dy	Maximum first derivative within 560–640	[39]
	Yellow edge area	SDy	Sum of first derivative values in yellow edge	[39]
	Blue edge amplitude	Db	Maximum first derivative within 490–530	[39]
	Blue edge area	SDb	Sum of first derivative values in blue edge	[39]
Vegetation index	Red edge ratio spectral index	RD	R <sub>740</sub> /R <sub>720</sub>	[40]
	Red edge model index	CI <sub>red-edge</sub>	(R <sub>780</sub> /R <sub>710</sub> ) - 1	[41]
	Normalized difference red edge index	NDRE	(R <sub>790</sub> R <sub>720</sub> )/(R <sub>790</sub> + R <sub>720</sub> )	[42]
	Normalized difference spectral index	ND705	(R <sub>750</sub> - R <sub>705</sub> )/(R <sub>750</sub> + R <sub>705</sub> )	[43]
	Near infrared ratio spectral index	NIR	R <sub>780</sub> /R <sub>740</sub>	[44]
Red edge ratio spectral index	RI-1 dB	R <sub>735</sub> /R <sub>720</sub>	[45]	

study, the number of hidden layer nodes was set to five, and the model was trained with five, eight, 10, 12, 16, and 20 hidden layer nodes. The training error is presented in Table 3. Prediction MRE is considered minimum when the number of hidden nodes is 10. Therefore, the number of hidden nodes was set to 10, the learning rate was 0.01, the number of iterations was 1000, and the maximum allowable error was 0.001. WNN was created using the MATLAB R2019b software (MathWorks, Inc. Natick, Massachusetts, USA).

According to the WNN theory, through repeated trainings and iteration, a WNN estimation model for petiole  $\text{NO}_3^-$ -N content in cotton under drip irrigation was developed based on spectral indices as shown in Fig. 2.

Random forest (RF) [46] is an algorithm that integrates multiple trees through ensemble learning and its basic unit is a decision tree. RF is commonly used in high-dimensional data classification and regression. The RF algorithm was developed using the MATLAB R2019b software. The number of classification trees in the RF algorithm was 1070.

The RBF neural network [46] can fit continuous non-linear functions, and its hidden layer adopts RBF, which

locally responds to input signals. In this study, the RBF neural network was developed using the MATLAB R2019b software. The variance parameter of RBF kernel function was set to 0.3.

The BP neural network [46] is a learning algorithm of feedback networks, that reflects input–output relationships of samples, and has a strong non-linear fuzzy approximation ability. In this study, a BP neural network was developed using the MATLAB R2019b software. The BP neural network adopts a three-layer structure, with 10 hidden layer nodes, 1000 iterations, and 0.01 learning rate.

**Results**

**The relationship between  $\text{NO}_3^-$ -N contents in petioles and trilateral parameters**

Table 4 shows that the correlation between  $\text{NO}_3^-$ -N content in petioles and blue edge parameters was stronger than that of red edge and yellow edge parameters. Although the correlations were significant; a negative correlation was observed among red edge amplitude (Dr), red edge area (SDr), yellow edge amplitude (Dy), and yellow edge area (SDy), while a positive correlation

**Table 3** Influence of the number of nodes in different hidden layers on network prediction error

Learning rate	Number of iterations	Maximum allowable error	Number of hidden layer nodes	MRE%
0.01	1000	0.001	5	7.14
0.01	1000	0.001	8	5.86
0.01	1000	0.001	10	5.82
0.01	1000	0.001	12	6.92
0.01	1000	0.001	16	6.35
0.01	1000	0.001	20	5.92

**Table 4** Correlation coefficient between  $\text{NO}_3^-$ -N content of petioles and trilateral parameters

Trilateral parameters	Correlation coefficients
Dr	-0.80**
SDr	-0.72**
Dy	-0.85**
SDy	-0.59**
Db	0.90**
SDb	0.90**

\*\*Means significant at the level of  $p < 0.01$

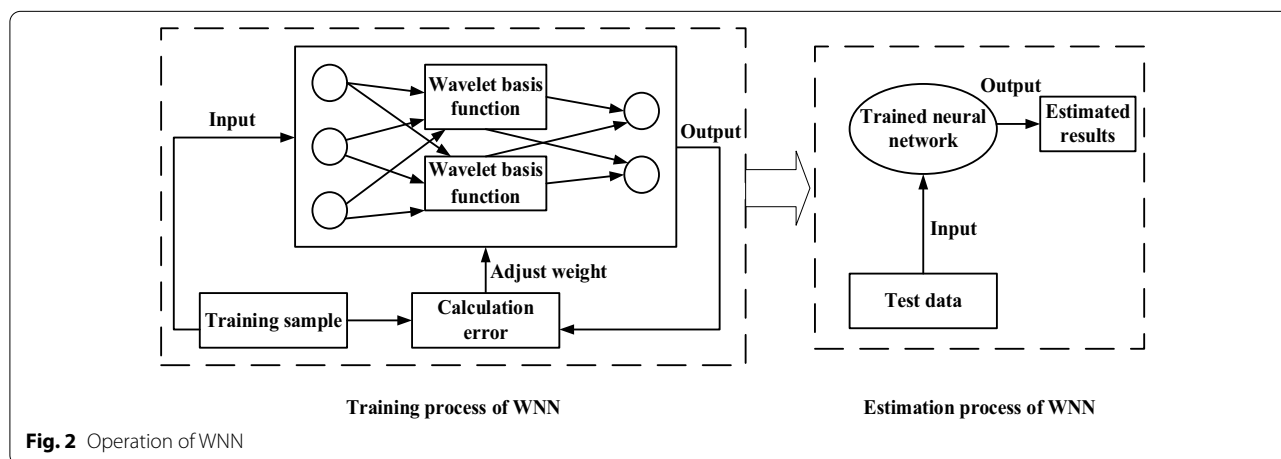


**Fig. 2** Operation of WNN

was observed between blue edge amplitude (Db) and blue edge area (SDb). Correlation coefficient of Db and SDb was 0.90.

From the regression analysis, Table 5 shows that blue edge parameters and petiole NO<sub>3</sub><sup>-</sup>-N content R<sup>2</sup> was higher while RMSE was lower when compared to those of red edge and yellow edge parameters. The polynomial regression equation of Db exhibited the highest coefficient of determination (R<sup>2</sup>=0.89), while the RMSE value of Db linear regression equation was the lowest (RMSE=1.04 g/L). Based on linear regression equations of blue edge, red edge and yellow edge parameters, the R<sup>2</sup> value of Db in blue edge parameters increased by 25.0% and 11.1%, respectively, when compared to Dr in red edge parameters and Dy in yellow edge parameters. Moreover, the R<sup>2</sup> value of SDb in blue edge parameters increased by 55.8% and 11.0%, respectively, when compared to SDr in red edge parameters and SDy in yellow edge parameters.

**Relationship between NO<sub>3</sub><sup>-</sup>-N content in petioles and vegetation indices**

Correlation analysis (Table 6) revealed a significant negative correlation between vegetation index red edge (RD) and NO<sub>3</sub><sup>-</sup>-N content in petioles, with a correlation coefficient of -0.81, followed by near infrared ratio spectral index (NIR), with a correlation coefficient of -0.79, and other vegetation indices that reached significant correlation levels (Table 6). Correlation analyses of NO<sub>3</sub><sup>-</sup>-N content in cotton petioles under drip irrigation and

**Table 6** Correlation coefficient between NO<sub>3</sub><sup>-</sup>-N content of petioles and vegetation indices

Type of reflectivity	Vegetation indices	Correlation coefficients
First derivative	RD	-0.85**
	CI <sub>red-edge</sub>	-0.89**
	NDRE	-0.80**
	ND705	-0.90**
	NIR	-0.62**
	RI-1 dB	-0.72**
Original	RD	-0.81**
	CI <sub>red-edge</sub>	-0.74**
	NDRE	-0.77**
	ND705	-0.76**
	NIR	-0.79**
	RI-1 dB	-0.77**

\*\*Means significant at the level of p < 0.01

vegetation indices developed based on the first six sets of derivative spectral data revealed that ND705 was significantly negatively correlated with NO<sub>3</sub><sup>-</sup>-N content in petioles, and the correlation coefficient was -0.90, followed by red edge model index (CI<sub>red-edge</sub>), with a correlation coefficient of -0.89 (Table 6). Correlation coefficients of ND705 and NO<sub>3</sub><sup>-</sup>-N contents in petioles were significantly increased by 18.4% and 20.3%, respectively except for NIR based on ND705 and CI<sub>red-edge</sub>.

**Table 5** Quantitative relationship between trilateral parameters and NO<sub>3</sub><sup>-</sup>-N content in petioles

Trilateral parameters	Functional model	Regression equation	R <sup>2</sup>	RMSE (g/L)
Dr	Linear	y = -1E + 06x + 21,084	0.64	1.40
	Exponential	y = 59,355e <sup>-160.9x</sup>	0.61	1.45
	Quadratic	y = -2E + 08x <sup>2</sup> + 6E + 06x - 23990	0.67	2.93
SDr	Linear	y = -12,321x + 13,673	0.52	2.28
	Exponential	y = 18,355e <sup>-1.876x</sup>	0.47	2.59
	Quadratic	y = -58,926x <sup>2</sup> + 48,072x - 895.38	0.60	2.53
Dy	Linear	y = -1E + 08x + 1114.1	0.72	1.08
	Exponential	y = 2691.4e <sup>-17931x</sup>	0.67	1.82
	Quadratic	y = -4E + 12x <sup>2</sup> - 5E + 08x - 9212.4	0.84	2.73
SDy	Linear	y = -193,244x - 1139.4	0.73	2.91
	Exponential	y = 1924.3e <sup>-29.42x</sup>	0.67	2.54
	Quadratic	y = -8E + 06x <sup>2</sup> - 905,730x - 16273	0.79	2.51
Db	Linear	y = 4E + 06x - 836.47	0.80	1.04
	Exponential	y = 2036.5e <sup>619.48x</sup>	0.72	1.50
	Quadratic	y = -3E + 09x <sup>2</sup> + 2E + 07x - 14359	0.89	1.64
SDb	Linear	y = 498,071x - 9405.9	0.81	1.45
	Exponential	y = 492.37e <sup>78.986x</sup>	0.80	1.53
	Quadratic	y = 9E + 06x <sup>2</sup> - 84,605x - 199.84	0.82	1.98

E stands for scientific counting; e is the base of natural logarithm

Regression analyses (Table 7) between  $\text{NO}_3^-$ -N contents in petioles and six vegetation indices during the key growth period of cotton under drip irrigation revealed that  $R^2$  values of the first derivative vegetation indices, RD,  $\text{CI}_{\text{red-edge}}$ , normalized difference red edge index (NDRE), and normalized difference spectral index (ND705) were higher than those of the original vegetation indices, and that RMSE values were lower than those of original vegetation indices. Among the three regression models, the  $R^2$  value of the polynomial regression

equation for the first derivative vegetation index, ND705 was the highest ( $R^2=0.83$ ), while the linear regression equation of the first derivative vegetation index,  $\text{CI}_{\text{red-edge}}$  had the lowest RMSE (0.92 g/L). In conclusion, the first derivative vegetation index, ND705 and  $\text{CI}_{\text{red-edge}}$  exhibited a higher predictive ability. The  $R^2$  value of the polynomial regression equation between ND705 and petiole  $\text{NO}_3^-$ -N content was 53.4% higher than that of ND705. The RMSE value of the linear regression equation of the first derivative vegetation index and petiole  $\text{NO}_3^-$ -N

**Table 7** Quantitative relationship between spectral indices and  $\text{NO}_3^-$ -N content

Type of reflectivity	Vegetation indices	Functional model	Regression equation	$R^2$	RMSE (g/L)
First derivative	RD	Linear	$y = -8116.9x + 13,150$	0.71	1.77
		Exponential	$y = 17,860e^{-1.306x}$	0.73	2.01
		Quadratic	$y = 3178.2x^2 - 13,332x + 15,120$	0.72	1.88
	$\text{CI}_{\text{red-edge}}$	Linear	$y = -76,288x - 66,089$	0.80	0.92
		Exponential	$y = 0.067e^{-12.01x}$	0.78	0.98
		Quadratic	$y = -169,389x^2 - 400,646x - 221,261$	0.80	0.93
	NDRE	Linear	$y = -27,424x - 18,368$	0.63	1.14
		Exponential	$y = 147.75e^{-4.115x}$	0.56	1.23
		Quadratic	$y = 126,872x^2 + 207,536x + 89,944$	0.67	1.18
	ND705	Linear	$y = -18,527x + 3265$	0.82	1.52
		Exponential	$y = 3707.4e^{-2.893x}$	0.78	1.35
		Quadratic	$y = -29,935x^2 - 30,687x + 2342.8$	0.83	1.69
	NIR	Linear	$y = -85,125x + 10,408$	0.39	1.45
		Exponential	$y = 11,137e^{-12.9x}$	0.35	1.55
		Quadratic	$y = -2E + 06x^2 + 47,910x + 8644.1$	0.44	1.44
	RI-1 dB	Linear	$y = -19,373x + 22,583$	0.52	2.37
		Exponential	$y = 78,853e^{-3.076x}$	0.52	2.91
		Quadratic	$y = 126,872x^2 + 207,536x + 89,944$	0.59	2.83
Original	RD	Linear	$y = -8564.7x + 25,826$	0.65	1.50
		Exponential	$y = 131,902e^{-1.36x}$	0.65	1.57
		Quadratic	$y = -10,788x^2 + 39,287x - 26,804$	0.67	1.47
	$\text{CI}_{\text{red-edge}}$	Linear	$y = -3415.6x + 14,222$	0.54	1.69
		Exponential	$y = 19,774e^{-0.516x}$	0.49	1.81
		Quadratic	$y = -357.75x^2 - 1914.2x + 12,720$	0.54	1.67
	NDRE	Linear	$y = -28,351x + 17,684$	0.59	1.70
		Exponential	$y = 34,790e^{-4.394x}$	0.56	1.81
		Quadratic	$y = -202,849x^2 + 124,311x - 10,381$	0.63	1.60
	ND705	Linear	$y = -2745.6x + 16,233$	0.58	2.38
		Exponential	$y = 29,232e^{-0.441x}$	0.59	2.41
		Quadratic	$y = -35.761x^2 - 2493x + 15,800$	0.58	2.34
	NIR	Linear	$y = -28,744x + 38,765$	0.62	1.66
		Exponential	$y = 946,939e^{-4.488x}$	0.60	1.81
		Quadratic	$y = -180,524x^2 + 369,826x - 180,634$	0.66	1.53
	RI-1 dB	Linear	$y = -10,960x + 28,560$	0.59	1.58
		Exponential	$y = 199,238e^{-1.729x}$	0.58	1.67
		Quadratic	$y = -26,273x^2 + 92,468x - 72,663$	0.64	1.52

E stands for scientific counting; e is the base of natural logarithm

content was 45.6% lower than that of the original vegetation index,  $CI_{red-edge}$ .

**Development and verification of the estimation models**

In this study, we used two stable and representative first derivative vegetation indices (ND705,  $CI_{red-edge}$ ) and Db as well as SDb (blue edge parameters) to develop the petiole  $NO_3^-$ -N content estimation model WNN. Simulated and measured values were fitted and analyzed using an independent validation test data. Results are presented in Table 8. The  $R^2$ , RMSE, and MAE values of the WNN estimation model based on first derivative vegetation indices were 0.81, 0.91 g/L, and 0.73 g/L, respectively, while the  $R^2$ , RMSE, and MAE values of the validation model were 0.82, 0.87 g/L, and 0.68 g/L, respectively. The  $R^2$ , RMSE, and MAE values of the WNN estimation model based on blue edge parameters were 0.88, 0.74 g/L and 0.58 g/L, respectively. The  $R^2$ , RMSE, and MAE values of the validation model based on blue edge parameters were 0.88, 0.65 g/L, and 0.47 g/L, respectively. The  $R^2$  value of WNN based on blue edge parameters was increased by 8.6%, whereas RMSE and MAE values were reduced by 18.7% and 20.5%, respectively, when compared to the estimation model based on first derivative vegetation indices. The  $R^2$  value of the validation model based on blue edge parameters was increased by 7.3%, whereas RMSE and MAE values were reduced by 25.2% and 30.9%, respectively, when compared to the estimation model based on first derivative vegetation indices. Generally, the  $R^2$  value of the validation model was higher than that of the estimation model, while RMSE and MAE values were lower

than those of the estimation model, implying that the validation model is stable.

The verification model of  $NO_3^-$ -N content in petioles was developed based on WNN, RF, RBF and BP (Table 9). The  $R^2$ , RMSE and MAE values of the WNN validation model based on first derivative vegetation indices were 0.82, 0.87 g/L, and 0.68 g/L. The  $R^2$  values of WNN, RF, and RBF were all 0.82. However, the RMSE and MAE values of WNN were 5.4% and 10.5% lower than those of RF, 1.0% and 5.6% lower than those of RBF, and 17.2% and 16.0% lower than those of BP, respectively. The  $R^2$ , RMSE, and MAE values of the WNN validation model based on blue edge parameters were 0.88, 0.65 g/L, and 0.47 g/L, respectively. Compared to RF, the  $R^2$  value of WNN was increased by 7.3%, whereas RMSE and MAE values were decreased by 17.7% and 21.7%, respectively. Compared to RBF, the  $R^2$  of WNN was increased by 8.6%, whereas RMSE and MAE values were decreased by 18.8% and 23.0%, respectively. Compared to BP, the  $R^2$  of WNN was increased by 14.3%, whereas RMSE and MAE values were decreased by 27.0% and 27.7%, respectively.

The  $R^2$  value of the WNN, based on blue edge parameters, increased by 7.3% while RMSE and MAE values reduced by 25.2% and 30.9%, respectively, when compared to the model based on first derivative vegetation indices. The RMSE and MAE values of the RF based on blue edge parameter values were reduced by 14.1% and 21.1%, respectively, when compared to the model based on first derivative vegetation indices. The RMSE and MAE values of the RBF based on blue edge parameter values were reduced by 9.1% and 15.3%, respectively, when compared to the model based on first derivative

**Table 8** Modeling and validation of  $NO_3^-$ -N content in petioles by wavelet neural network

Spectral index type	Modeling				Validation			
	Number of samples	$R^2$	RSME (g/L)	MAE (g/L)	Number of samples	$R^2$	RSME (g/L)	MAE (g/L)
Vegetation indices	60	0.81	0.91	0.73	60	0.82	0.87	0.68
Blue edge parameters	60	0.88	0.74	0.58	60	0.88	0.65	0.47

**Table 9** Validation between predicted and measured of  $NO_3^-$ -N content in petioles based on different methods

Methods	Blue edge parameters				Vegetation indices			
	Number of samples	$R^2$	RSME (g/L)	MAE (g/L)	Number of samples	$R^2$	RSME (g/L)	MAE (g/L)
WNN	60	0.88	0.65	0.47	60	0.82	0.87	0.68
RF	60	0.82	0.79	0.60	60	0.82	0.92	0.76
RBF	60	0.81	0.80	0.61	60	0.82	0.88	0.72
BP	60	0.77	0.89	0.65	60	0.74	1.02	0.81



vegetation indices. The  $R^2$  value of BP based on blue edge parameters was increased by 4.1% while RMSE and MAE values were reduced by 12.7% and 19.8%, respectively, when compared to the model based on first derivative vegetation indices.

## Discussion

### Feasibility of remote sensing monitoring $\text{NO}_3^-$ -N content in cotton petioles under drip irrigation

Timely and accurate monitoring of N contents in crops is key to accurate application of N fertilizer [47]. Advances in remote sensing technology present a potential novel method for monitoring crop nutrition [48]. This technology has been used to monitor plant N contents and N accumulation, although studies on  $\text{NO}_3^-$ -N contents in cotton petioles under drip irrigation are scarce [49]. Monitoring of petiole  $\text{NO}_3^-$ -N contents is widely used to evaluate crop nutrition and to inform top-dressing [48]. In this study, the correlations among six trilateral parameters, six vegetation indices, and  $\text{NO}_3^-$ -N contents in cotton petioles under drip irrigation was revealed that a large proportion of the spectral index was strongly correlated with  $\text{NO}_3^-$ -N content in petioles. Among them, correlation coefficients of Db, SDb, and first derivative ND705 are all 0.90. These findings imply that estimation of  $\text{NO}_3^-$ -N contents in cotton petioles under drip irrigation using spectral indices is feasible.

### Potential of blue edge parameters for the estimation of $\text{NO}_3^-$ -N content in petioles

Trilateral parameters, especially red edge parameters, effectively reflect the characteristics of crop N status [49, 50]. Studies on wheat, rice, and other crops developed N content estimation models based on red edge parameters, which achieved satisfactory results [51, 52]. In this study, we established that the correlation between blue edge parameters and petiole  $\text{NO}_3^-$ -N contents was strong, and that the traditional regression model of blue edge parameters and petiole  $\text{NO}_3^-$ -N content was superior to the red edge and yellow edge parameters. Estimation and validation models based on blue edge parameters and WNN exhibited a superior capacity to the vegetation index model based on the red edge band. This finding is relatively inconsistent with the findings of most previous studies, which focused on the correlation between red edge parameters and crop N. Blue edge is sensitive to crop N. Li et al. [53] determined N levels in winter wheat by performing hyperspectral analyses, and established that blue-violet light was sensitive to N. Stroppiana et al. [54] reported that the blue light is the ideal wave segment for N estimation in rice. Our findings could be attributed to variations in crop canopy structure

and biomass, the unique climatic conditions in Xinjiang, drip irrigation fertilization methods, or to other factors.

When selecting spectral characteristic parameters, most of the studies have evaluated red edge parameters and paid less attention to the blue edge parameters, which cover wavelengths between 490 and 530 nm. Therefore, blue edge parameters should be considered when determining N levels based on spectral data. We also showed the potential of blue edge parameters in estimating of N levels in crops.

### Applications of neural networks in remote sensing monitoring

The  $R^2$  value of the WNN estimation and verification models were relatively high, while RMSE and MAE values were relatively low as shown in Tables 8, 9, implying that stability of the model is high while its estimation capacity is superior. Combined WNN maintains the advantages of artificial neural networks and wavelet analysis, which accelerates network convergence, thereby preventing the algorithm from falling into local optimum and occasionally making local analysis more frequent [55, 56]. The RBF neural network [57] algorithm confers the advantages of rapid training and convergence speed, strong input-output mapping ability, and strong generalization ability when compared to the BP neural network algorithm. Furthermore, our findings confirmed that the estimation model based on the RBF neural network is superior to that of the BP neural network model.

Neural networks [58, 59] exhibit a great potential in learning and developing non-linear complex relationship models, and they exhibit high tolerance for input objects. Wang et al. [60] constructed the Chinese cabbage population quality BP neural network model which effectively monitors, N utilization of Chinese cabbage is monitored effectively. The constructed population quality evaluation model has a high  $R^2$  value and a comparatively low RMSE value for quality evaluation of Chinese cabbage in different periods. Sabzi et al. [61] used the hyperspectral imaging technology combined with artificial neural networks and imperialist competition algorithm (ANN-ICA) to detect early excessive N levels in cucumber leaves. They found that hyperspectral imaging technology combined with artificial neural networks can detect excess N in plants in near infrared band (NIR), and the correct classification rate is 96.11%. Neural networks can better simulate heteroscedasticity and have the ability to learn hidden relations in data without imposing any fixed relations [57, 64].

Studies on crop physiological parameter estimation have shown that the RF algorithm exhibits a high accuracy and estimation ability, and confers the advantages of strong stability and high efficiency when compared with

other modeling methods. Loozen et al. [62] used the RF technology estimate the N content of a European forest canopy, which exhibited a superior accuracy ( $R^2=0.62$ ,  $RMSE=0.18$ ). To establish an efficient method for estimating winter wheat biomass, Yue et al. [63] used RF algorithm to develop a regression model of winter wheat biomass by combining spectrum, radar backscattering, vegetation index, and radar vegetation index, they found that the stochastic forest algorithm can be applied in remote sensing to estimate the winter wheat biomass. The RF regression algorithm has been shown to result in over fitting and higher test errors when compared to the neural network algorithm [64, 65].  $RMSE$  and  $MAE$  values of WNN and RBF models based on the vegetation indices were found to be lower than those of the RF during model validation (Fig. 3). The  $R^2$  value of WNN based on blue edge parameters was higher than that of the RF, while  $RMSE$  and  $MAE$  values were lower than those of the RF (Fig. 4), consistent with previous findings that the RF method exhibits a weak predictive ability.

### Conclusions

We analyzed and compared the performance of trilateral parameters and vegetation indices in estimating  $NO_3^-$ -N contents in cotton petioles under drip irrigation, in addition to determining an effective method for estimating  $NO_3^-$ -N contents in cotton petioles under drip irrigation using blue edge parameters and WNN. It was found that the correlation between blue edge parameters and petiole  $NO_3^-$ -N content was 0.90, and the regression equation of blue edge parameters and petiole  $NO_3^-$ -N content had a higher  $R^2$  and a lower  $RMSE$ . The validation model, which was based on blue edge parameters and WNN, exhibited the highest coefficient ( $R^2=0.88$ ), lowest root mean square error ( $RMSE=0.65$  g/L) and lowest mean absolute error ( $MAE=0.47$  g/L). Therefore, blue edge parameters and WNN can be used to estimate  $NO_3^-$ -N contents in cotton petioles under drip irrigation.

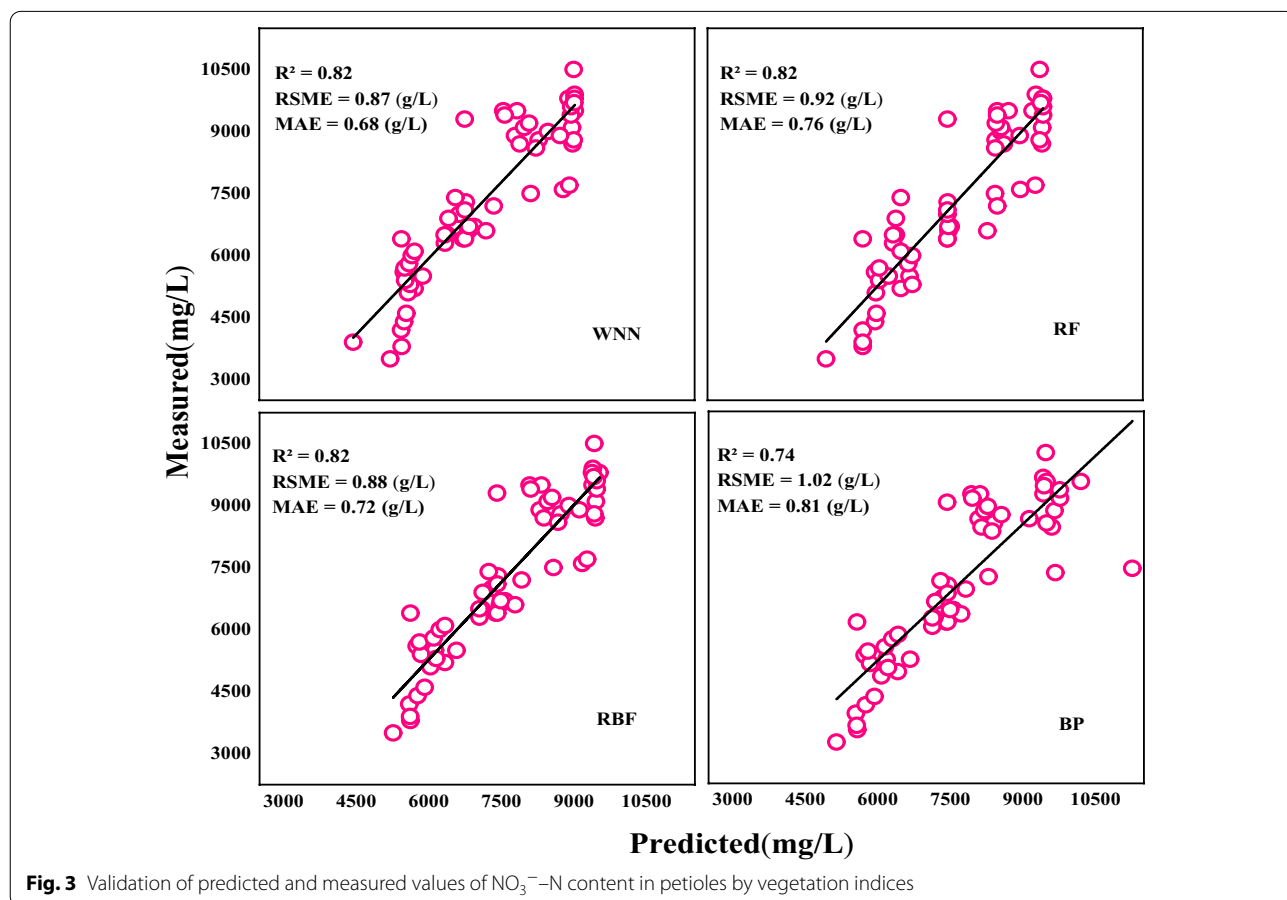


**Fig. 3** Validation of predicted and measured values of  $NO_3^-$ -N content in petioles by vegetation indices

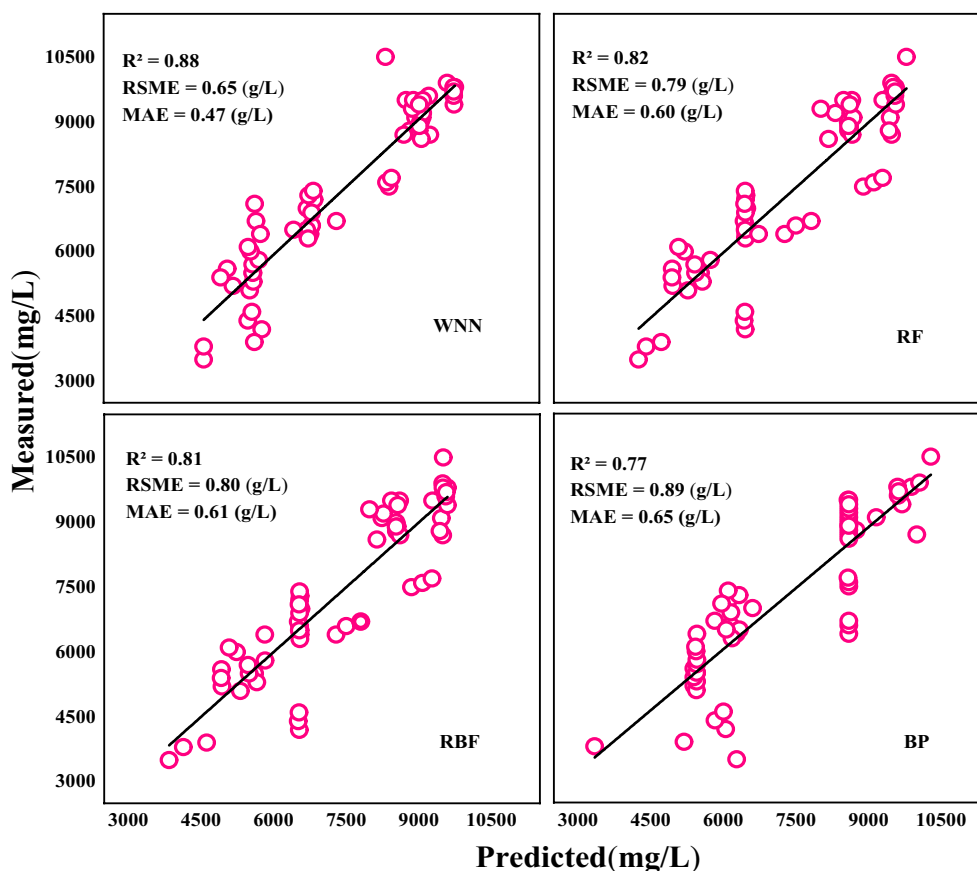


**Fig. 4** Validation of predicted and measured values of  $\text{NO}_3^-$ -N content in petioles by blue edge parameters

#### Acknowledgements

We thank the National and local joint engineering research center of information management and Application Technology for modern agricultural production (XPCC) for the experiments.

#### Authors' contributions

ZD contributed to the conceptualization, methodology, software, data curation, writing—original draft preparation, writing—reviewing and editing. YL and FM contributed to the writing—reviewing and editing, supervision, project administration, funding acquisition. BC, MW, ML, XL, XF, SW contributed to the investigation, data curation, resources. All authors read and approved the final manuscript.

#### Funding

This study was supported by the National Natural Science Foundation of China (31860346), the Key Technologies and System Construction of Big Data in Main Links of Cotton Production of XPCC (2018Aa00400), the Financial Science And Technology Plan Project of XPCC (2020Ab017, 2020Ab018), the Financial Science And Technology Plan Project of Shihezi City (2020ZD01) and Autonomous Region Postgraduate Research and Innovation Project (XJ2019G082).

#### Availability of data and materials

The remotely sensed and field sampling data used in this study is available from the corresponding author on reasonable request.

#### Declarations

##### Ethics approval and consent to participate

All authors read and approved the manuscript.

##### Consent for publication

All authors agreed to publish this manuscript.

##### Competing interests

The authors declare that they have no known competing financial interests or personal relationships that could have appeared to influence the work reported in this paper.

##### Author details

<sup>1</sup>School of Agriculture, Shihezi University, Shihezi 832003, Xinjiang, People's Republic of China. <sup>2</sup>National and Local Joint Engineering Research Center of Information Management and Application Technology for Modern Agricultural Production (XPCC), Shihezi 832003, People's Republic of China.

Received: 5 April 2021 Accepted: 2 August 2021

Published online: 18 August 2021

#### References

1. Rochester IJ, Constable GA. Nitrogen-fertiliser application effects on cotton lint percentage, seed size, and seed oil and protein concentrations. *Crop Pasture Sci.* 2020;71:831–6.

2. Li YY, Gao XP, Tenuta M, Gui DW, Li XY, Xue W, Zeng FJ. Enhanced efficiency nitrogen fertilizers were not effective in reducing N<sub>2</sub>O emissions from a drip-irrigated cotton field in arid region of Northwestern China. *Sci Total Environ.* 2020;748:141543.
3. Yang XY, Geng JB, Huo XQ, Lei ST, Lang Y, Li H, Liu QJ. Effects of different nitrogen fertilizer types and rates on cotton leaf senescence, yield and soil inorganic nitrogen. *Agron Soil Sci.* 2020. <https://doi.org/10.1080/03650340.2020.1799983>.
4. Echer FR, Cordeiro CFD, de la Torre EDR. The effects of nitrogen, phosphorus, and potassium levels on the yield and fiber quality of cotton cultivars. *J Plant Nutr.* 2020;43:921–32.
5. Wei CZ, Zhang FS, Zhu HM, Hou ZA, Guo GS, Bao BY. Study on nitrogen nutrition diagnosis and topdressing recommendation of cotton in Xinjiang. *Chinese J Agric Sci.* 2002;1500–1505.
6. Wang LS, Aziz K, Yuan Y, Wu YY, Shah AN, Tung S, Yang GZ. Effects of sowing date and density on NO<sub>3</sub><sup>-</sup>-N content in cotton petioles and roots. *Acta Cotton Sin.* 2016;28:574–83.
7. Darnell RL, Stutte GW, Sager JC. Nitrate concentration effects on NO<sub>3</sub><sup>-</sup>-N uptake and reduction, growth, and fruit yield in strawberry. *J Am Soc Hortic Sci.* 2001;126:560.
8. Brito DDMCD, Santos CD, Goncalves FV, et al. Effects of nitrate supply on plant growth, nitrogen, phosphorus and potassium accumulation, and nitrate reductase activity in crambe. *J Plant Nutr.* 2013;36:275–83.
9. Wu SH, Liu JF, Cheng JY. Study on nitrate nitrogen in cotton petioles as a diagnostic index of nitrogen nutrition. *Hubei Agric Sci.* 1987;19–22.
10. Carlson RM, Cabrera RI, Paul JL, Quick J, Evans RY. Rapid direct determination of ammonium and nitrate in soil and plant tissue extracts. *Commun Soil Sci Plant Anal.* 1990;21:1519–29.
11. Singh D, Singh K, Hundal HS, Sekhon KS. Diagnosis and recommendation integrated system (driis) for evaluating nutrient status of cotton (*Gossypium hirsutum*). *J Plant Nutr.* 2006;29:113–25.
12. Qu P, Xu WH. Crop nutrition and computer vision technology. *Wirel Pers Commun.* 2020;117(2):887–99.
13. Rosolem CA, van Mellis V. Monitoring nitrogen nutrition in cotton. *Rev Bras Ciênc Solo.* 2020;34:1601–7.
14. Woodson WR, Boodley JW. Petiole nitrate concentrations as an indicator of geranium nitrogen status. *Commun Soil Sci Plant Anal.* 1983;14:363–71.
15. Keisling TC, Mascagni NJ, Maples RL, Thompson KC. Using cotton petiole nitrate nitrogen concentration for prediction of cotton nitrogen nutritional status of a clayey soil. *J Plant Nutr.* 1995;18:35–45.
16. Saranga Y, Landa A, Shekel Y. Near-infrared analysis of cotton leaves as a guide for nitrogen fertilization. *Agron J.* 1998;90(1):16–21.
17. Boggs JL, Tsegaye TD, Coleman TL. Relationship between hyperspectral reflectance, soil nitrate-nitrogen, cotton leaf chlorophyll, and cotton yield: a step toward precision agriculture. *J Sustain Agric.* 2003;22:5–16.
18. Banerjee BP, Spangenberg G, Kant S. Fusion of spectral and structural information from aerial images for improved biomass estimation. *Remote Sens.* 2020;12(19):3164.
19. Liu N, Zhao R, Qiao L. Growth stages classification of potato crop based on analysis of spectral response and variables optimization. *Sensors.* 2020;20:3995.
20. Chang CY, Zhou R, Kira O. An Unmanned Aerial System (UAS) for concurrent measurements of solar-induced chlorophyll fluorescence and hyperspectral reflectance toward improving crop monitoring. *Agric For Meteorol.* 2020;294:108145.
21. Abulaiti Y, Sawut M, Maimaitiaili B, Ma CY. A possible fractional order derivative and optimized spectral indices for assessing total nitrogen content in cotton. *Comput Electron Agric.* 2020;171:105275.
22. Rao NR, Garg PK, Ghosh SK, Dadhwal VK. Estimation of leaf total chlorophyll and nitrogen concentrations using hyperspectral satellite imagery. *J Agric Sci.* 2020;154:112699.
23. Gautam RK, Panigrahi S. Image processing techniques and neural network models for predicting plant nitrate using aerial images. In: IEEE international joint conference on neural networks. 2003;1031–1036.
24. Yadav VP, Prasad R, Bala R, Srivastava PK. Assessment of red-edge vegetation descriptors in a modified water cloud model for forward modelling using Sentinel-1A and Sentinel-2 satellite data. *Int J Remote Sens.* 2021;42:794–804.
25. Dalen M, Tubana B, Kanke Y. Relationship of red and red-edge reflectance-based vegetation indices with stalk and fiber yield of energy cane harvested at different dates. *Arch Agron Soil Sci.* 2019;66:1888–907.
26. Hansen PM, Schjoerring JK. Reflectance measurement of canopy biomass and nitrogen status in wheat crops using normalized difference vegetation indices and partial least squares regression. *Remote Sens Environ.* 2003;86:542–53.
27. Railyan VY, Korobov RM. Red edge structure of canopy reflectance spectra of triticale. *Remote Sens Environ.* 1993;46:173–82.
28. Gilabert MA, Gandía S, Meliá J. Analyses of spectral-biophysical relationships for a corn canopy. *Remote Sens Environ.* 1996;55:11–20.
29. Feng S, Xu TY, Yu FH, Chen CL, Yang X, Wang NY. Research of method for inverting nitrogen content in canopy leaves of Japonica rice in North-eastern China based on hyperspectral remote sensing of unmanned aerial vehicle. *Spectrosc Spectr Anal.* 2019;39:3281–7.
30. Xiu LN, Zhang H, Guo QZ, Wang ZH, Liu XN. Estimating nitrogen content of corn based on wavelet energy coefficient and BP neural network. In: 2015 2nd international conference on information science and control engineering. 2015;212–216.
31. Anshuka A, Buzacott AJV, Vervoort RW, van Ogtrop FF. Developing drought index based forecasts for tropical climates using wavelet neural network: an application in Fiji. *Theor Appl Climatol.* 2020;143(1):557–69.
32. Minjae L, Hyemi K, Hee-Joung K. Sparse-view CT reconstruction based on multi-level wavelet convolution neural network. *Physica Med.* 2020;80:352–62.
33. Jouila A, Nouri K. An adaptive robust nonsingular fast terminal sliding mode controller based on wavelet neural network for a 2-DOF robotic arm. *J Franklin Inst.* 2020;357:13259–82.
34. Ghoddusi H, Creamer GG, Rafizadeh N. Machine learning in energy economics and finance: a review. *Energy Econ.* 2019;81:709–27.
35. Rosolem CA, van Mellis V. Monitoring nitrogen nutrition in cotton. *Revista Brasileira De Ciencia Do Solo.* 2010;34:1601–7.
36. Liu XF, Zhang Z, Lv X, Nie YB. Establishment of nitrogen topdressing model for drip irrigation spring wheat based on nitrate. *Xinjiang Agric Sci.* 2017;54:27–32.
37. Xia WH, Liu T, Guan Y, Wang J, Chu GX. Comparison of nitrate reflectometer and SPAD method in nitrogen nutrition diagnosis of maize. *Chinese J Ecol Agric.* 2016;24:1339–46.
38. Horler DNH, Dockray M, Barber J. The red edge of plant leaf reflectance. *Int J Remote Sens.* 1983;4:273–88.
39. Wang XP, Zhang F, Kung HT, Yu HY. Spectral response characteristics and identification of typical plant species in Ebinur lake wetland national nature reserve (ELWNNR) under a water and salinity gradient. *Ecol Ind.* 2017;81:222–34.
40. Vogelmann JE, Rock BN, Moss DM. Red edge spectral measurements from sugar maple leaves. *Int J Remote Sens.* 1993;14:1563–75.
41. Gitelson AA, Vina A, Ciganda V. Remote estimation of canopy chlorophyll content in crops. *Geophys Res Lett.* 2005. <https://doi.org/10.1029/2005GL022688>.
42. Barnes EM, Clarke TR, Richards SE. Coincident detection of crop water stress, nitrogen status and canopy density using ground based multi-spectral data. Bloomington, MN, USA. In: Proceedings of the fifth international conference on precision agriculture. 2000;1619.
43. Gitelson A, Merzlyak MN. Spectral reflectance changes associated with autumn senescence of *Aesculus hippocastanum* L. and *Acer platanoides* L. leaves. Spectral features and relation to chlorophyll estimation. *J Plant Physiol.* 1994;143:286–92.
44. Misteale B, Schmidhalter U. Tractor-based quadrilateral spectral reflectance measurements to detect biomass and total aerial nitrogen in winter wheat. *Agron J.* 2010;102:499–506.
45. Gupta R, Vijayan D, Prasad T. Comparative analysis of red-edge hyperspectral indices. *Adv Space Res.* 2003;32:2217–22.
46. Zhou ZH. Machine learning. Beijing: Tsinghua University Press; 2015.
47. Kodur S, Shrestha UB, Maraseni TN. Environmental and economic impacts and trade-offs from simultaneous management of soil constraints, nitrogen and water. *J Clean Prod.* 2019;222:960–70.
48. Wu JD, Wang D, Rosen CJ. Comparison of petiole nitrate concentrations, SPAD chlorophyll readings, and Quick Bird satellite imagery in detecting nitrogen status of potato canopies. *Field Crop Res.* 2015;101:96–103.
49. Lu J, Miao Y, Shi W. Developing a proximal active canopy sensor-based precision nitrogen management strategy for high-yielding rice. *Remote Sens.* 2020;12:1440.

50. Wheeler KI, Levia DF, Vargas R. Visible and near-infrared hyperspectral indices explain more variation in lower-crown leaf nitrogen concentrations in autumn than in summer. *Oecologia*. 2020;192:13–27.
51. Cao Q, Miao YX, Li F, Gao XW, Liu B, Lu DJ, Chen XP. Developing a new Crop Circle active canopy sensor-based precision nitrogen management strategy for winter wheat in North China Plain. *Precis Agric*. 2017;18(1):2–18.
52. Jiang J, Zhang ZY, Cao Q, Liang Y, Krienke B, Tian YC, Zhu Y, Cao WX, Liu XJ. Use of an active canopy sensor mounted on an unmanned aerial vehicle to monitor the growth and nitrogen status of winter wheat. *Remote Sens*. 2020;12(22):3684.
53. Li F, Miao Y, Hennig SD. Evaluating hyperspectral vegetation indices for estimating nitrogen concentration of winter wheat at different growth stages. *Precis Agric*. 2010;11:335–57.
54. Stroppiana D, Boschetti M, Brivio PA. Plant nitrogen concentration in paddy rice from field canopy hyperspectral radiometry. *Field Crop Res*. 2009;111:119–29.
55. Ghamariadyan M, Imteaz MA. A wavelet artificial neural network method for medium term rainfall prediction in Queensland (Australia) and the comparisons with conventional methods. *Int J Climatol*. 2020;41:E1396–416.
56. Dong YH, Fu ZT, Peng YQ, Zheng YJ, Yan HJ, Li XX. Precision fertilization method of field crops based on the wavelet-BP neural network in China. *J Clean Prod*. 2019;246:118735.
57. Basheer IA, Hajmeer M. Artificial neural networks: fundamentals, computing, design, and application. *J Microbiol Methods*. 2000;43:3–31.
58. Salehi M, Farhadi S, Moieni A, Safaie N, Hesami M. A hybrid model based on general regression neural network and fruit fly optimization algorithm for forecasting and optimizing paclitaxel biosynthesis in *Corylus avellana* cell culture. *Plant Methods*. 2021;17:1–13.
59. Yang S, Zheng LH, He P, Wu TT, Sun S, Wang MJ. High-throughput soybean seeds phenotyping with convolutional neural networks and transfer learning. *Plant Methods*. 2021;17:1–17.
60. Wang QL, Mao XY, Jiang XS, Pei DD, Shao XH. Digital image processing technology under backpropagation neural network and K-Means Clustering algorithm on nitrogen utilization rate of Chinese cabbages. *PLoS ONE*. 2021;16:e0248923.
61. Taghadomi-Saberi S, Masoumi AA, Sadeghi M, Zekri M. Integration of wavelet network and image processing for determination of total pigments in bitter orange (*Citrus aurantium* L.) peel during ripening. *J Food Process Eng*. 2019;42:e13120.1–e13120.8.
62. Loozen Y, Rebel KT, de Jong SM, Lu M, Ollinger SV, Wassen MJ, Karsenberg D. Mapping canopy nitrogen in European forests using remote sensing and environmental variables with the random forests method. *Remote Sens Environ*. 2020;247:111933.
63. Yue J, Yang GJ, Feng HK. Comparison of remote sensing estimation models for winter wheat biomass based on Stochastic Forest algorithm. *Agric Eng*. 2016;32:175–82.
64. Leo B. Random forests. *Mach Learn*. 2001;45:5–32.
65. Han ZY, Zhu XC, Fang XY, Wang ZY, Wang L, Zhao GX, Jiang YM. Hyperspectral estimation of Lai in Apple crown based on SVM and RF. *Spectrosc Spectr Anal*. 2016;36:800–5.

## Publisher's Note

Springer Nature remains neutral with regard to jurisdictional claims in published maps and institutional affiliations.

Ready to submit your research? Choose BMC and benefit from:

- fast, convenient online submission
- thorough peer review by experienced researchers in your field
- rapid publication on acceptance
- support for research data, including large and complex data types
- gold Open Access which fosters wider collaboration and increased citations
- maximum visibility for your research: over 100M website views per year

At BMC, research is always in progress.

Learn more [biomedcentral.com/submissions](https://biomedcentral.com/submissions)

